

1 **The application of diffusive gradients in thin films (DGT) for improved understanding of metal**  
2 **behaviour at marine disposal sites**

3

4 Ruth Parker<sup>1</sup>, Thi Bolam<sup>1\*</sup>, Jon Barry<sup>1</sup>, Claire Mason<sup>1</sup>, Silke Kröger<sup>1</sup>, Lee Warford<sup>1</sup>, Briony Silburn<sup>1</sup>,  
5 Dave Sivyer<sup>1</sup>, Silvana Birchenough<sup>1</sup>, Andrew Mayes<sup>2</sup> and Gary R. Fones<sup>3</sup>

6 <sup>1</sup> Centre for Environment, Fisheries and Aquaculture Science, Lowestoft Laboratory, Pakefield Road,  
7 Lowestoft, Suffolk, UK, NR33 0HT.

8 <sup>2</sup>School of Chemistry, University of East Anglia, Norwich Research Park, Norwich, UK, NR4 7TJ

9 <sup>3</sup>School of Earth and Environmental Sciences, University of Portsmouth, Burnaby Building, Burnaby  
10 Road, Portsmouth, UK, PO1 3QL.

11 \* Corresponding author. Tel.: +44 1502 524525; E-mail address: thi.bolam@cefas.co.uk

12

13 **Abstract:**

14 Assessment of the effects of sediment metal contamination on biological assemblages and function  
15 remains a key question in marine management, especially in relation to disposal activities. However,  
16 the appropriate description of bioavailable metal concentrations within pore-waters has rarely been  
17 reported. Here, metal behaviour and availability at contaminated dredged material disposal sites within  
18 UK waters were investigated using Diffusive Gradient in Thin films (DGT). Three stations, representing  
19 contrasting history and presence of dredge disposal were studied. Depth profiles of five metals were  
20 derived using DGT probes as well as discrete analysis of total metal concentrations from sliced cores.  
21 The metals analysed were: iron and manganese, both relevant to sediment biogeochemistry; cadmium,  
22 nickel and lead, classified as priority pollutants. DGT time-integrated labile flux profiles of the metals  
23 display behaviour consistent with increasingly reduced conditions at depth and availability to DGT (iron  
24 and manganese), subsurface peaks and a potential sedimentary source to the water column related to  
25 the disposal activity (lead and nickel) and release to pore-water linked to decomposition of enriched  
26 phytodetritus (cadmium). DGT data has the potential to improve our current understanding of metal  
27 behaviour at impacted sites and is suitable as a monitoring tool. DGT data can provide information on  
28 metal availability and fluxes within the sediment at high depth-resolution (5 mm steps). Differences  
29 observed in the resulting profiles between DGT and conventional total metal analysis illustrates the  
30 significance of considering both total metals and a potentially labile fraction. The study outcomes can  
31 help to inform and improve future disposal site impact assessment, and could be complemented with  
32 techniques such as Sediment Profile Imagery for improved biological relevance, spatial coverage and  
33 cost-effective monitoring and sampling of dredge material disposal sites. Additionally, the application  
34 of this technology could help improve correlative work on biological impacts under national and  
35 international auspices when linking biological effects to more biologically relevant metal  
36 concentrations.

37 **Key words:** Dredge material, disposal, metal profiles, sediments, DGT (Diffusive Gradient in Thin-  
38 films), labile, bioavailability.

39

## 40 **1.0 Introduction:**

41 Dredging operations are conducted to remove sediments in order to maintain harbour berths, marinas  
42 and channels. The amount of dredging and disposal undertaken worldwide varies depending on a  
43 combination of economic, social and legislative needs. This activity is controlled under national and  
44 international legislations via licensing authorities, which also have a duty to comply with international  
45 conventions on dredging, disposal and marine environmental protection to minimise any adverse  
46 environmental consequences (Birchenough et al., 2006; Birchenough et al., 2010).

47 There are 136 sites currently designated for dredged material disposal around the coast of  
48 England, mostly in close proximity to the coast and major ports or estuaries. Individual quantities  
49 disposed, may range from a few hundred to several million tonnes, with an approximate annual sum of  
50 40 million tonnes (Bolam et al., 2010a and 2010b). The nature of the disposed material may vary from  
51 soft silts to boulders or even crushed rock according to origin (capital material), although the majority  
52 consists of finer material (maintenance dredge material). Disposed material may have differing  
53 sediment types, higher loads of organic material and, although regulated, a higher associated loads of  
54 various contaminants such as organics or metals, from background or reference sediments. Disposal  
55 sites within the UK are selected for annual monitoring based on a tier-based approach that classifies the  
56 number of possible issues or environmental concerns that may be associated with dredged material  
57 disposal to sea at certain sites (Bolam et al., 2010b). In licensing the disposal of dredged material at  
58 sea, several national and international agreements (e.g., the London Protocol of 1996 (LP96), the  
59 OSPAR Convention, the Habitats and Species Directive (92/43/EEC), the Wild Birds Directive  
60 (79/409/EEC), the Water Framework Directive (2000/60/EC) and the Waste Framework Directive  
61 (2008/98/EC)), must be taken into account, to determine whether likely impacts arising from the  
62 dredging and disposal are acceptable (MEMG, 2003). Criteria considered under the various  
63 conventions and directives include the presence and levels of contaminants in the materials to be  
64 disposed of, along with perceived impacts on any sites of conservation value in the vicinity of disposal.

65 A number of different substances are determined as part of the monitoring of disposal sites,  
66 such as tributyltin, polycyclic aromatic hydrocarbons, organohalogenes (e.g. PCBs) and metals measured  
67 as total metal concentrations in bulk sediments. Additional physico-chemical information, such as  
68 sediment particle size, organic carbon and nitrogen content, and sediment profile imagery (SPI), is  
69 obtained to further characterise sediment status (Birchenough et al., 2006; Bolam et al., 2010a and b).

70 Existing monitoring programmes are designed to address important questions such as: what is  
71 the fate of contaminants (including metals) imported to the site with the disposed material and what  
72 effect does this have on ecological components? Associated questions are those relating to the disposed  
73 sediments as sources and sinks of metals to the water column, either by diffusion or due to disturbance

74 by storms. At present, the analysis of total metals is the traditional technique used to assess the metal  
75 contaminant pressure within the disposal site monitoring programmes. In comparison, little is known  
76 regarding metal speciation or detailed vertical distribution and partitioning of metal contaminants  
77 between pore-water and solid phases within the sediments at the disposal sites. As such, the impact  
78 assessment of disposed material and management accordingly can be limited by using a total metal  
79 approach alone in assessing metal pressure within the sediment.

80 The sediment pore-water concentrations of contaminants and hence the bioavailability of  
81 chemicals in sediments is often estimated using various techniques (Forstner and Wittman, 1981;  
82 Bufflap and Allen, 1995; Stockdale et al., 2009). Pore-water can be obtained by *ex-situ* (slicing,  
83 centrifuge, suction, or pressure) methods or *in situ* (probe pumping or diffusion) methods, such as  
84 passive samplers (dialysis peepers, teflon sheets, DET and DGT). *Ex-situ* methods are often difficult to  
85 control and analyse due to issues in controlling oxidation during sampling, preservation and detection  
86 limits associated with small volumes and lack of pre-concentration. Additionally, as samples are  
87 handled open to the air, whilst on the boat, issues such as clean handling techniques can be a challenge  
88 for standard monitoring conditions. There may also be limitations of sampling resolution (Bufflap and  
89 Allen, 1995). Diffusion methods such as passive samplers (Peijnenburg et al., 2014) can be useful in  
90 that they can offer high resolution and are constrained inside probes which can allow cleaner handling,  
91 without full clean trace metal provisions. Some techniques can also pre-concentrate chemicals which  
92 can facilitate analysis success by lowering detection limits. Deployment times are typically  $\geq 24$  h, but  
93 deployments for this length of time can also minimise the effect of disturbances caused by deployment  
94 (Davison et al. 2007). Passive sampling methods can provide ‘dissolved’ concentrations in sediment  
95 porewater ( $C_{\text{free}}$ ) thus providing a more relevant exposure metric for risk assessment than do total  
96 concentrations (Peijnenburg et al. 2014). Other information that can be obtained from passive samplers  
97 in sediments includes estimates of metal sources, sinks and time-integrated measurements.

98 Passive samplers such as Diffusive Gradient in Thin Films (DGT) have been used increasingly  
99 in sediments to determine pore-water metal ‘dissolved’ concentrations ( $C_{\text{DGT}}$ ) and time-integrated labile  
100 metal fluxes (Zhang et al. 1995; Davison et al. 2000; Fones et al. 2001; Fones et al. 2004; Peijnenburg  
101 et al. 2014; Amato et al. 2015). DGT is a passive sampling technique that has been used for determining  
102 metal concentrations in natural waters for more than 20 years (Davison and Zhang; 1994). A typical  
103 DGT device for common divalent metal ions consists of Chelex<sup>®</sup>-100 resin embedded within a  
104 hydrogel, overlaid with a diffusive layer of hydrogel and a filter membrane. These devices have been  
105 successfully employed in the sampling of metals prior to analysis of their concentrations in surface  
106 waters (Schintu et al. 2010; Shiva et al. 2016), soils (Oporto et al. 2009; Ernstberger et al. 2005) and  
107 sediments (Davison et al. 1997; Fones et al. 2004; Tankere-Muller et al. 2007; Teal et al., 2009; Teal et  
108 al., 2013) and by using different binding agents the range of determinands has been extended to include

109 other cations (Dahlqvist et al. 2002), oxyanions (Panther et al. 2014) and targeted species including  
110 sulphide (Teasdale et al. 1999) and uranium (Turner et al. 2012; Turner et al. 2015).

111 DGT is a well-developed technique for sampling metals in bulk water, with deployments from  
112 6 to 72 h being typical, with the rate of metal uptake by the resin gel controlled by the diffusive layer  
113 (Davison and Zhang, 2012). The diffusion coefficient in the diffusive gel is similar to that of the  
114 diffusion rate of the metal ion in pure water and can be measured accurately by experiment (Zhang and  
115 Davison 1999). Diffusion coefficients for many metals including different species (Metal-NOM  
116 complexes) in polyacrylamide gels are available in the literature (Zhang and Davison, 2000; Scally et  
117 al. 2006; Shiva et al. 2015). The concentration in the water can then be calculated using the previously  
118 published DGT equation (Davison and Zhang, 1994; Davison and Zhang, 2012). One problem  
119 associated with this is the potential for metal species and complexes operationally defined as 'labile' to  
120 be sorbed onto the resin gel, this thus depends on the relative diffusion rates of the species that pass  
121 through the gel (Zhang and Davison, 2000).

122 DGT has also been fully characterized for use in sediments (Zhang et al. 1995; Fones et al.  
123 2004; Amato et al. 2014). When used in sediments it is an in-situ technique that provides time-integrated  
124 measurements of the combined labile metal fluxes from the sediment pore water and particulate phases  
125 (Zhang et al. 1995). Upon deployment of the DGT probe in the sediment, metals dissolved in the pore  
126 water are rapidly accumulated on the resin in the binding gel. This generates a localized zone of  
127 depletion in the pore waters and induces a release of labile, weakly bound metals absorbed onto  
128 sediment particles (Harper et al. 1998; Ciffroy et al. 2011). The DGT device thus acts as a localised  
129 sink, removing labile metal species permanently from solution. The metal continuously accumulates in  
130 the DGT device while it is deployed in the sediment (Harper et al. 1999) and therefore measures a time-  
131 averaged flux from the pore water to the resin (Harper et al 1998 and 1999).

132 Harper et al. (1998) and Zhang et al. (1995) both showed that DGT fluxes can be interpreted as  
133 pore water concentrations using Fick's law of diffusion along with metal diffusion coefficients,  
134 deployment time and diffusive gel thickness if the metal concentrations at the interface between the  
135 DGT device and sediment are well buffered by metal resupply from the sediment solid phase. However,  
136 in most cases there is only partial resupply or resupply by metal diffusion so DGT measurements are  
137 the result of dynamic equilibriums between the binding strength of the DGT resin and that of the  
138 sediment (Davison and Zhang, 2012). Amato et al. (2015) suggested that interpreting DGT  
139 measurements as fluxes ( $\mu\text{g}/\text{h}/\text{m}^2$ ) is the most suitable approach for sediment deployments. The DGT  
140 metal flux will differ depending on sediment properties and also the chemical behaviour of the metals.  
141 These differing release rates will influence accumulation of metals by benthic organisms thus providing  
142 the use of DGT-metal fluxes for assessing metal bioavailability in sediments (Simpson et al., 2012;  
143 Amato et al. 2014; Amato et al. 2015). However, only a few studies have utilised DGT sediment

144 measurements in the context of contamination studies at capping (Knox et al., 2012; Knox et al., 2016)  
145 or disposal sites.

146 While the established practise of analysing total trace metals in bulk sediment samples gives  
147 important information about absolute concentrations and so potential hazards, looking at depth resolved  
148 profiles of metal fluxes as measured by DGT improves our understanding of how mobile and thus  
149 available these metals are from a total disposal reservoir. In other words, what actual risk disposed  
150 sediments pose. The bioavailability of heavy metals has been more closely linked to levels of dissolved  
151 contaminants in pore-waters than to bulk sediment concentrations (Calmano et al., 1993; Ankley et al.,  
152 1996b; Chapman et al., 1998; Eggleton and Thomas, 2004) as bioavailability and toxicity of metals in  
153 sediments was not well predicted by sediment metal concentrations only (Lee and Lee, 2005).

154 The aim of this work was to apply therefore a passive sampling approach, diffusive gradient in  
155 thin films (DGT) technology, as a complementary tool to the routine monitoring conducted at an UK  
156 disposal site and thus assess the additional insight and understanding of metal behaviour and fate gained  
157 by including this technique in a monitoring programme. Some of the metals examined (lead, nickel and  
158 cadmium) are on the EU Water Framework Directive (WFD) list of priority substances and OSPAR list  
159 of priority pollutants while others have mainly ecological relevance (iron and manganese).

160

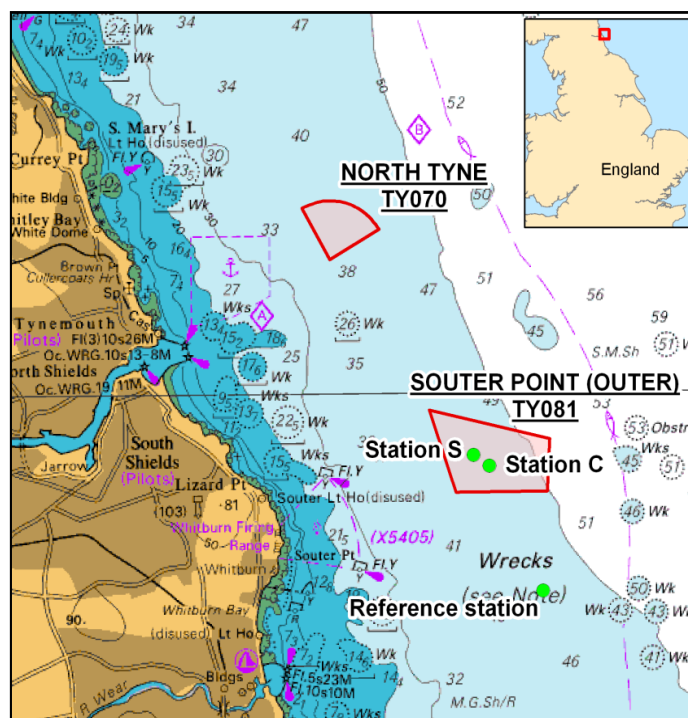
## 161 **2.0 Materials and methods**

### 162 *2.1 Study site*

163 The Souter Point disposal site is located off the North East coast of the UK (Figure 1). This site has  
164 been used for the disposal of dredged material since 1952 and selected stations have been monitored  
165 annually since the early 1970s (Bolam et al., 2010a; Bolam et al., 2010b). The site is located at a depth  
166 of approximately 40-50 m, shallowing by up to 5m towards the western boundary due to historical  
167 accumulations of minestone and fly-ash deposits (Rees et al., 2006). Tidal currents in the vicinity of  
168 the disposal site are moderate in strength and run generally parallel to the coastline, with a southerly  
169 net residual drift. The sediments within the vicinity of this disposal site are muddy sands. However,  
170 sediments may vary to a large extent following dredged material disposal and in relation to a sites earlier  
171 history of solid industrial wastes and other discharges inshore (Rowlatt, et al., 1989; Rowlatt and  
172 Ridgeway, 1997; Birchenough et al., 2007). The results of this work summarises results obtained during  
173 a research cruise conducted in June 2011. Observations and measurements were made during the cruise  
174 and on recovered samples back at the laboratory.

### 175 *2.2 Sampling approach*

176 A 0.1 m<sup>2</sup> NIOZ box-core was used to collect sediment at 3 stations: 4 core replicates were collected  
177 from the Reference station (located to the south of the disposal site) and 3 core replicates were taken  
178 from each of stations C and S, both located within the disposal site (Figure 1).



179

180 Figure 1. Souter Point disposal and sampling stations on the disposal stations (S, C) and reference  
 181 station (R).

182

183 The DGT devices for metals in sediments were purchased as complete assembled probes from DGT  
 184 Research (Lancaster, UK). The overall dimensions are 5 x 240 x 40 mm, with an exposure window of  
 185 18 x 150 mm and the device consists of a 0.8 mm APA diffusive gel, polyethersulphone filter membrane  
 186 and Chelex binding layer. Probes and procedural blanks were de-oxygenated in a 0.01M NaCl solution  
 187 overnight using oxygen free-nitrogen. The cores were placed in an incubating tank (in the dark and  
 188 filled with oxygenated seawater) on-board ship and were stabilised for 2 hours before deployment of  
 189 the probes. For each core, two probes were used: the Chelex gel probe (for metals determination) and  
 190 the silver-iodine (AgI) gel probe (for sulphide determination). The probes were inserted into the  
 191 sediment core, leaving 1 - 2 cm between the top of the probe window and the sediment/water interface.  
 192 Furthermore, Chelex gel discs and AgI gel discs were deployed in the incubating tank in parallel with  
 193 the probes to determine concentrations in the overlying water column. The probes and discs were  
 194 deployed for 24 - 28 hrs. The time and temperature were recorded at the deployment and retrieval  
 195 points. On removal, nanopure water (resistivity of 18.2 MΩ·cm) was used to rinse off any sediment  
 196 traces that remained on the surface of the probes/discs. These were stored in a labelled bag and kept in  
 197 the refrigerator prior to transfer to the laboratory for analysis.

198 Five replicate Sediment Profile Imagery (SPI) images were taken at each of the sites where the  
 199 DGT technique was employed. Sediment Profile Imagery is a rapid, *in-situ* technique, which takes  
 200 vertical profile pictures of the upper 20cm of the sediment system. The SPI camera works like an

201 ‘inverted periscope’, the camera possesses a wedge-shaped prism with a Plexiglas faceplate and an  
202 internal light provided by a flash strobe. The back of the prism has a mirror mounted at a 45° angle  
203 which reflects the image of the sediment-water interface at the faceplate up to the camera. The imaging  
204 system (a Nikon D-100 camera) provides *in-situ* visualisation of sediment characteristics (layers,  
205 structure) and the interaction of the sediment and succession of large in-fauna (Rhoads and Germano,  
206 1982; Germano et al., 2011). Visual assessment of sediment colour can be used to assess sediment redox  
207 state, in particular iron reduction (loss of brown), manganese reduction (grey) and pyrite formation  
208 (black), (Lyle, 1983; Bull and Williamson., 2001; Teal et al., 2009; Teal et al., 2010).

209

### 210 2.3 Analysis of passive samplers

211 *Chelex gel*: The DGT probes were rinsed with nano-pure water once retrieved. After opening the  
212 window frame, the filter and diffusive gel layer were removed and discarded. The remaining resin gel  
213 layer was carefully placed on a flat surface and the gel was sliced at 0.5 cm resolution. Each slice was  
214 then placed in a sample tube and 1 ml of 1M HNO<sub>3</sub> was added to the tube, ensuring that the resin gel  
215 layer was fully immersed in the HNO<sub>3</sub> solution. The sample was left to elute for at least 24 hours before  
216 analysis (Davison *et al.*, 2007). The eluted solution was then diluted prior to analysis by Inductively-  
217 Coupled Plasma-Mass Spectrometry (ICP-MS) using an Agilent 7500ce (Agilent Technologies,  
218 Waldbronn, Germany), and by Inductively-Coupled Plasma-Atomic Emission Spectroscopy (ICP-  
219 AES) using a Varian Ax Vista Pro (Agilent Technologies, Waldbronn, Germany). Quantification of  
220 Cd, Fe, Mn, Ni, and Pb was performed by external calibration and deploying eight levels (0, 0.5, 1, 5,  
221 10, 20, 100 and 500µg/L) of working standard solutions which were prepared from a customised mixed  
222 metal standard solution of 100mg/L (SPEX Certiprep Ltd, Middlesex, UK). The limits of quantification  
223 (LOQ) for each metal DGT analysis (24hr deployment) are (nmol/cm<sup>2</sup>/s): Cd; 2.8x10<sup>-8</sup>, Pb: 1.14x10<sup>-8</sup>,  
224 Ni: 5.7x10<sup>-8</sup>, Fe: 9.7x10<sup>-6</sup>, Mn: 1.6x10<sup>-7</sup>.

225

226 *AgI gel*: The AgI gels were removed from the probes and covered with a polyester film. The gels were  
227 then scanned while wet in a flat-bed scanner. The greyscale intensity of the scanned images was  
228 analysed with the software Image J (<http://rsb.info.nih.gov/ij/>). Using the calibration curve derived by  
229 Teasdale *et al.*, 1999, total dissolved sulphides can be quantitatively measured in the gel.

230

231 *Metal flux calculations*: The measured concentrations,  $C_g$  (µg kg<sup>-1</sup>) of the DGT gel solutions were  
232 converted to molar concentrations and used to calculate the mass,  $M$  (nmol cm<sup>-2</sup>), accumulated in the  
233 resin layer of each gel strip:

234

$$235 \quad M = \left( \frac{C_g (v + V)}{0.8 \times A} \right) \frac{1}{x} \quad (1)$$

236 where  $V$  is the volume of gel (mL),  $v$  the extractant volume (mL) and  $x$  the atomic mass of the element  
237 in question. The factor 0.8 accounts for the fact that only 80% of the bound metal is released (Davison  
238 et al. 2000). Knowing the time of gel deployment,  $t$  (sec), allowed calculation of the time averaged Flux  
239  $F$  ( $\text{nmol cm}^{-2} \text{s}^{-1}$ ) of metal from the porewaters to the resin strip,

240

$$241 \quad F = \frac{M}{t \times A} \quad (2)$$

242

243 where  $A$  is the area of exposed gel ( $\text{cm}^2$ ). The term ‘flux’ used from here onwards thus refers to the flux  
244 of reduced metal forms from the pore water to the resin gel of the DGT device, here onwards referred to  
245 as ‘resin gel’ (i.e. not reduction fluxes or process rates) and serves as a proxy for metal availability.

246

#### 247 *2.4 Supporting sediment analysis*

248 Supporting measurements to complement the DGT probes and characterise the sediment at each of the  
249 stations were also collected. Oxygenation of the upper sediments layer was measured using oxygen  
250 pore water profiles obtained on intact cores and using oxygen microelectrodes (Unisense, Denmark)  
251 and a method adapted from Rabouille et al. (2001). Sediment characteristics were derived from vertical  
252 slices of sub-cores from a NIOZ box-corer at resolutions 0 to 0.5 cm, 0.5 to 1 cm and then at 1 cm  
253 intervals, stored at  $-20^\circ \text{C}$  or analysed immediately. These sample slices were analysed for particle size,  
254 porosity, chlorophyll/phaeopigment and total organic carbon content.

255 Particle size analysis (PSA) was conducted using a method developed by Mason et al. (2011).  
256 In short, a subsample of each sediment was screened at 1 mm and laser sized using a Malvern  
257 Mastersizer 2000 (Malvern, Worcestershire, UK). The remaining sample was wet split at 1 mm, and  
258 the  $> 1$  mm sediment was oven dried and then dry sieved over a range of test sieves down to 1 mm.  
259 Sediment  $< 1$  mm was oven dried and weighed. The results from these analyses were combined to  
260 provide a full particle size distribution. Summary statistics, including % gravel, % sand and % mud,  
261 were derived from the full distribution dataset. Total Organic Carbon (TOC) was analysed using broadly  
262 similar methodology to that described by Verardo et al., 1990. Samples were freeze-dried and then  
263 ground to homogenise the sample. Inorganic carbonate was removed from a 1.3 g subsample using  
264 sulphurous acid to excess. Sub-samples ( $\sim 0.5$  g) were then weighed into tin cups and analysed using a  
265 Carlo Erba EA1108 Elemental Analyser. Chlorophyll a and phaeopigments were extracted in 90%  
266 acetone (Fisher Scientific, Leicestershire, UK) and refrigerated before analysis. A Turner Designs  
267 Model 10AU filter fluorometer (Turner Designs, Sunnyvale, California, USA) was used to measure  
268 extracted chlorophyll a by fluorescence before and after acidification, as described in Sapp et al. 2010.  
269 The fluorometer was calibrated using a solution of pure chlorophyll a (Sigma-Aldrich, St. Louis) with  
270 the concentration being determined spectrophotometrically. The percentage error of chlorophyll a  
271 analyses was  $< 2\%$  relative to Turner-certified reference material. Porosity was calculated using the



272 dry weights and wet weights of known volumes of sediment slices assuming a sediment particle density  
273 of  $2.7 \text{ g cm}^{-3}$  and a seawater density of  $1.035 \text{ g cm}^{-3}$  (Sapp et al. 2010).

274

### 275 *2.5 Total Metals*

276 A sub-core from each station was taken and sliced according to its visual description. Each slice was  
277 subsequently analysed for total metals on the  $< 63 \mu\text{m}$  sediment fraction. Typically, 0.2 g of the sieved  
278 and freeze-dried sediment sample was digested in a mixture of hydrofluoric (HF), hydrochloric and  
279 nitric acids using enclosed vessel microwave heating. The HF was then neutralised by the addition of  
280 boric acid and the digest made up in 1 % nitric acid and further diluted prior to analysis by ICP-MS and  
281 ICP-AES. Quantification of Cd, Fe, Mn, Ni, and Pb used external calibration with Indium as internal  
282 standard. A method blank and a certified reference material (CRM) PACS-2 (a marine sediment  
283 produced by the National Research Council Canada) were run within each sample batch so that the day-  
284 to-day performance of the method could be assessed. Shewhart control charts were derived from the  
285 CRM data and monitored using (upper/lower) warning and control limits set at  $\pm 2$  and 3 standard  
286 deviations from the mean value, respectively. Any batches with results outside these control limits were  
287 rejected and the samples re-analysed. The mean recoveries of all elements of interest range from 94%  
288 to 116% with a % relative standard deviations ranging from 2.8% to 12.2%.

289

### 290 *2.6 Statistical approaches and analysis*

291 To aid in comparing and contrasting features of DGT profiles within and between sites, a statistical  
292 model was fitted to each of the metal profiles. Before the main analysis, mean values were taken over  
293 the replicates to avoid statistical complications caused by spatial correlations between the cores. When  
294 examining the profiles, natural logs (Ln) were taken to reduce the visual impact on the profile of large  
295 readings. The Ln data also better fitted the assumptions behind the modelling which followed.

296 Initially, Ln profile plots of all eight metals were completed at all sites. For metals exhibiting the biggest  
297 differences between sites (Pb, Ni, Mn and Fe), further modelling was conducted to tease out the  
298 statistical evidence for these differences. We describe this modelling below.

299 The depth profiles for each of the metals at the three stations was smoothed using a Generalised  
300 Additive Model (GAM) (Wood, 2006) using the R package mgcv (R Development Core Team, 2010).  
301 Thin plate regression splines were used to smooth the data and the degree of smoothing (number of  
302 degrees of freedom (df) for the model parameters) was set to the minimum needed to explain the main  
303 fluctuations in the profile: we used 5 df for Pb and Mn and 4 df for Ni and Fe. The residuals (data minus  
304 the smoothed value) were calculated at each of the observed depths. For Pb and Ni, autocorrelation  
305 plots suggested that neighbouring residuals were independent; however, residuals from the Mn and Fe  
306 profiles were correlated. Thus, two different kinds of models, one assuming independence and one  
307 assuming one-lag auto correlation were required to model the depth profiles.

308 For the independent residuals, for a particular site and at each depth  $i$ , we assume that data arises from  
 309 the model:

$$310 \ln(M_i) = s_i + e_i \quad (3)$$

311 where  $s_i$  is the smoothed value from the GAM model of metal  $M_i$ , and  $e_i$  is an independent error term  
 312 which we assume to be distributed  $N(0, \sigma^2)$ , where  $\sigma^2$  is the variance of points around the smoothed  
 313 line  $\sigma^2$  is estimated by the sum of the squared residuals divided by  $(n - k)$ , where  $n$  is the number  
 314 of points and  $k$  is the number of degrees of freedom used in fitting the GAM model.

315 For the autocorrelated models, an autoregressive model of order 1 was used to the model the residuals:

$$316 r_i = \alpha r_{i-1} + e_i \quad (4)$$

317 where  $r_i$  is the  $i$ th residual,  $\alpha$  is a parameter (estimated by maximum likelihood using the *ar* function  
 318 in R) and  $e_i$  is an independent error term as in model (3). Simulated realisations of  $M_i$  were generated  
 319 from (4) by adding on the smoothed surface  $s_i$ .

320 One thousand realisations were then simulated from the model in (3) or (4) and the mid 95% envelope  
 321 taken. This is equivalent to a 95% confidence interval for the profile at each depth (Manly, 2008).

322

### 323 3.0 Results and discussion

#### 324 3.1 Bulk metal and sediment characteristics

325 A summary of station sediment characteristics is shown in Table 1a and b and Figure 2 and bulk  
 326 sediment metal profiles are illustrated in Figure A.1 (Appendix 1).

327

328 Table 1a: Mean sediment characteristics from sliced sediment cores (0 to ~10cm). Number in brackets  
 329 is one standard deviation.

330

Station	Silt/clay ( $<63 \mu\text{m}$ , %)	Porosity	Chlorophyll ( $\text{mg}/\text{m}^3$ )	Phaeo- pigment ( $\text{mg}/\text{m}^3$ )	TOC (% mass/ mass)	Oxygen penetration (OPD) - cm
Reference	17.0 (3.7)	0.45 (0.04)	3.0 (2.3)	14.0 (7.0)	1.3 (0.3)	0.5 (0.2)
Disposal S	49.2 (20.7)	0.62 (0.05)	3.4 (2.4)	14.2 (6.9)	5.6 (1.6)	0.4 (0.2)
Disposal C	22.4 (16.9)	0.53(0.05)	4.7 (3.9)	14.7 (7.4)	5.4 (0.9)	0.4 (0.1)

331

332

333

334

335

336

337

338

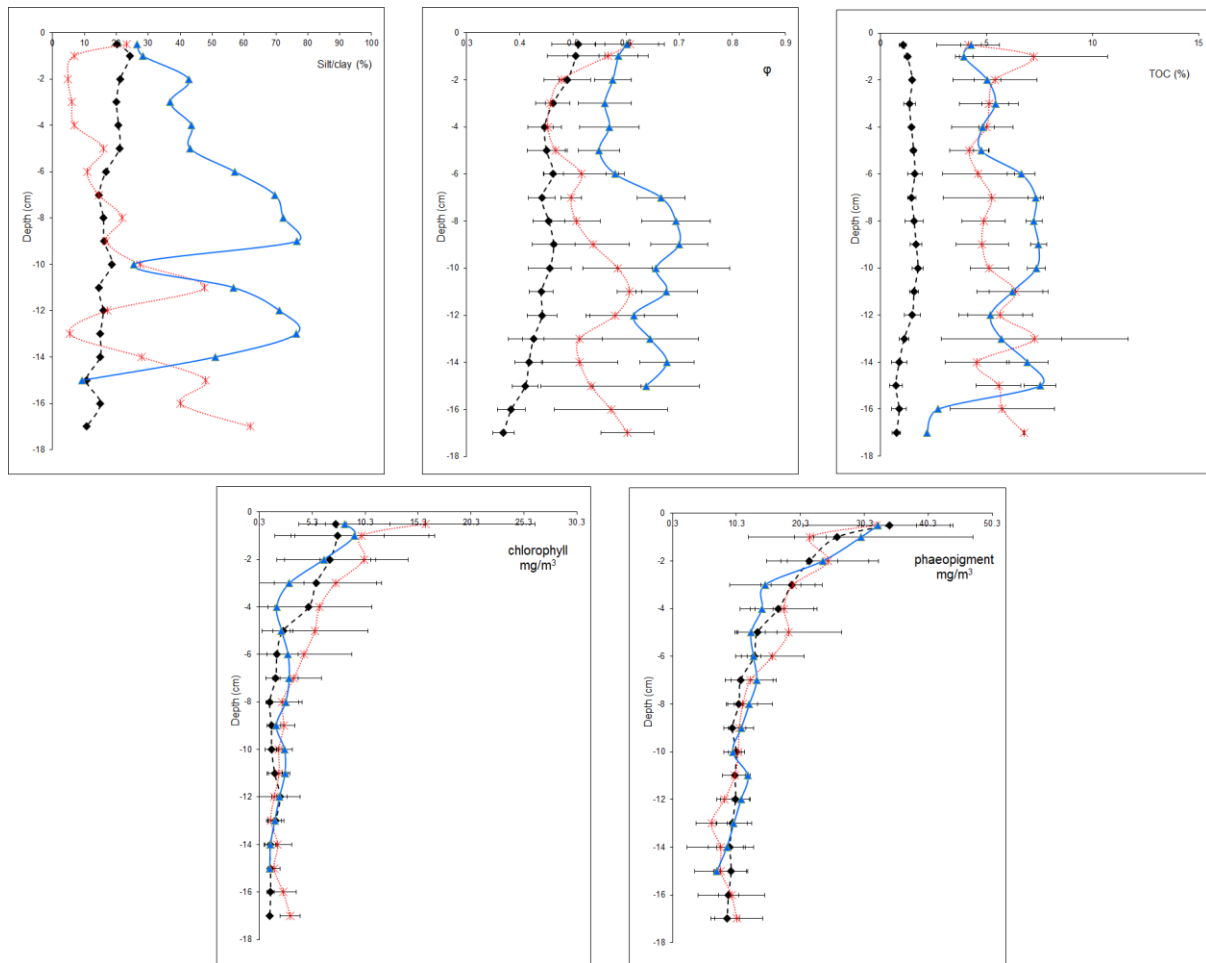
339

340 Table 1b: Mean total metal concentration from bulk samples from core layers (full plots are in Appendix  
 341 1 Figure A.1)  
 342

Average Concentrations <sup>#</sup>	Ni (mg/kg)	Cd (mg/kg)	Pb (mg/kg)	Mn (mg/kg)	Fe (g/kg)
Reference (n=4)	50.0	<0.18	136	445	38.9
Disposal C (n=7)	49.6	0.50	172	510	39.6
Disposal S (n=6)	50.6	0.46*	164	475	39.1

343 \*Cd at layer 8-9cm <0.2mg/kg

344 <sup>#</sup>SD not available as single measurement at each layer.



345

346 Figure 2: Vertical profiles of sediment properties at the three stations (reference, station C and station  
 347 S) Silt/clay (%), Porosity, Total Organic carbon (%m/m), Chlorophyll and  
 348 Phaeopigment. Error bars are +/- 1 standard deviation, n=3

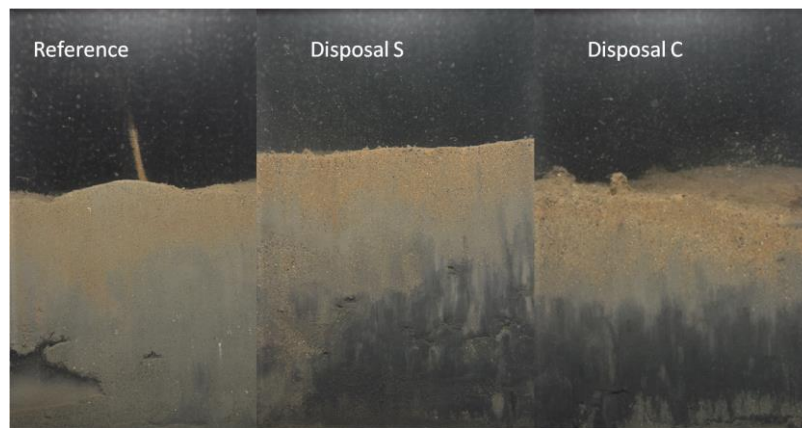
349

350 All stations were composed of either muddy sands where the sand:mud (mud being defined as the  
 351 sediment fraction  $<63\mu\text{m}$ , and sand between  $63\mu\text{m}$  and  $2\text{mm}$ ) ratio is  $>1:1$  and  $<9:1$ ; or to a lesser extent  
 352 sandy muds, where the sand:mud ratio is  $>1:9$  and  $<1:1$ ; as defined in Folk classification (Folk, 1954).  
 353 Note all bulk samples contained  $<2\%$  gravel and therefore for the purposes of these descriptions this  
 354 has been ignored. Porosity in the upper layers of the sediment at the reference station was lowest (0.45)  
 355 and elevated at the disposal stations, especially in the deeper sediment layers. Total organic carbon was  
 356 lowest at the Reference station with higher total organic carbons ( $> 5\%$  m/m) at the two disposal  
 357 stations. The sediment characteristics depth profiles (Figure 2) illustrate the differences between the  
 358 reference and disposal stations. The reference station showed a gradual decrease in porosity and organic  
 359 carbon with depth whilst the disposal stations exhibited complex porosity and carbon signatures down-  
 360 core probably related to disposal events. The heterogeneous structure in vertical profiles illustrated the  
 361 contrasting disposal events at the impacted stations at different depths and with differing % silt/clay,  
 362 TOC and porosity signatures. Station C in particular exhibited a low % silt/clay level in the upper parts  
 363 of the sediment. The pigment profiles are similar across the stations and illustrate the water column

364 source with similar degradation profiles with depth. The oxygen profiles and penetration depth were  
365 similar for all the stations, with diffusion-type profiles and with oxygen consumed within the upper 1 cm  
366 of the sediment. Observations conducted on the SPI images using  $\text{Fe}^{3+}$  colour also showed that more  
367 reduced sediment conditions were found deepest at the reference station, and shallowest at the disposal  
368 stations (Figure 3). The SPI images also showed the occurrence of sulphide formation (black  
369 colouration) to be more intense and shallower in the disposal station sediments when compared to the  
370 reference station and this supports an assessment of increased reducing conditions at these sites.

371

372



373

374 Figure 3: Example Sediment Profile Images (SPI) from the three stations at Souter Point (size of SPI  
375 optical window is 15 cm wide by 20 cm deep).

376

377

### 378 3.2 DGT fluxes and profiles

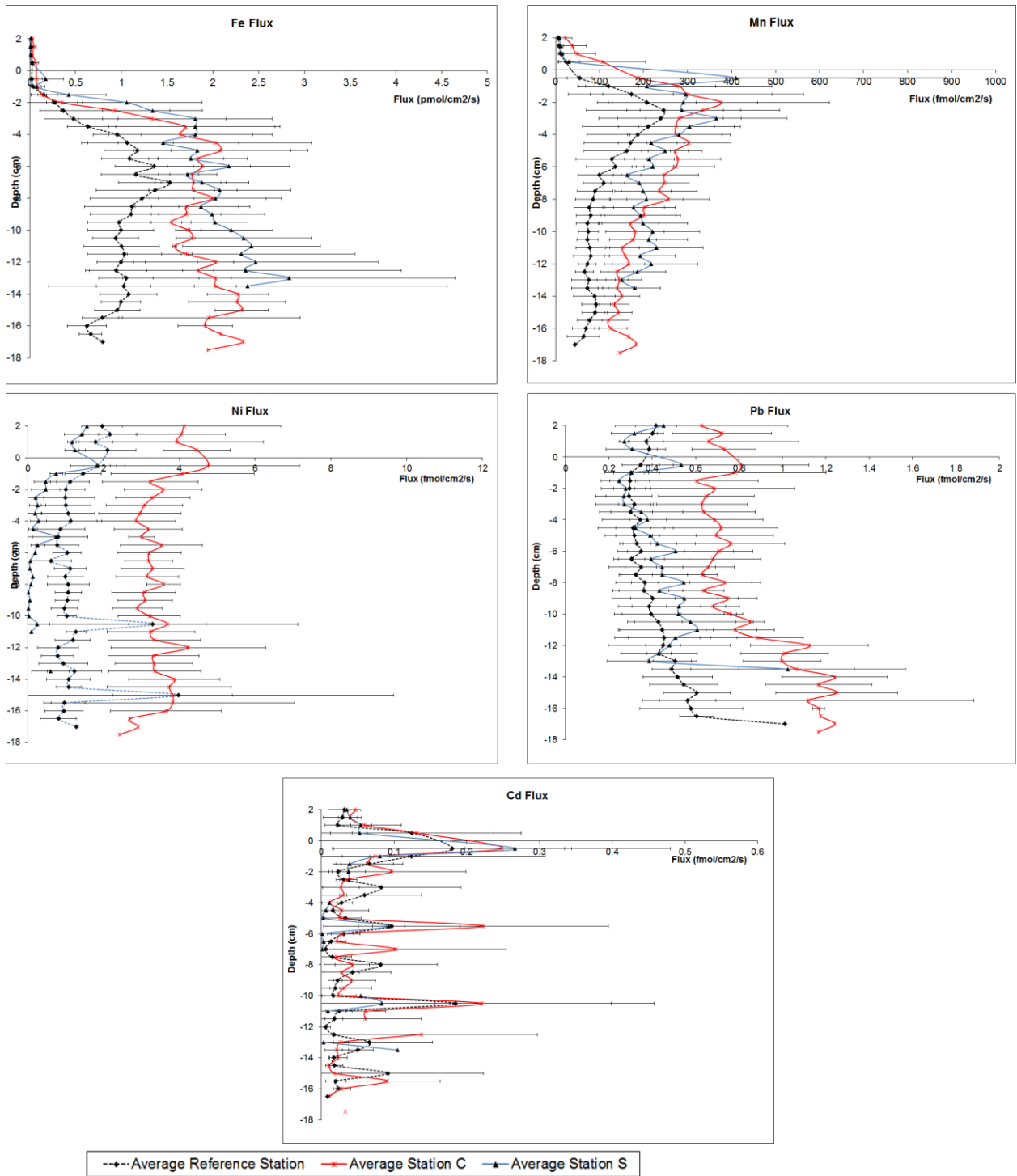
379 DGT metal fluxes were calculated for each of the deployed DGT probes at each station according to  
380 the method described in Davison and Zhang (1994) and the average flux profiles ( $\pm$ sd) were plotted  
381 for each metal at the 3 stations (Figure 4).

382

### 383 3.3 Metal sediment behaviour

384 **Iron and Manganese:** The DGT flux profiles showed high resolution information of iron (Fe) and  
385 manganese (Mn) remobilisation behaviours. Both metals are redox sensitive and are used as successive  
386 Terminal Electron Acceptors (TEAs) during the remineralisation of organic matter, Mn before Fe  
387 (Burdige, 2006). Their supply to the resin gel increased as they became reduced in the sediments ( $\text{Fe}^{3+}$   
388 to  $\text{Fe}^{2+}$ ,  $\text{Mn}^{4+}$  to  $\text{Mn}^{2+}$ ). Consistent with this, Fe and Mn DGT flux profiles (Figure 4) showed the start  
389 of sub-surface remobilisation at about 1 – 2 cm and < 1 cm, respectively. Mn release occurred as oxygen  
390 was depleted within the upper centimetre of the sediment. Iron supply to the resin gel rapidly increased  
391 near the surface, but below the oxic zone. This close linkage between Fe and Mn behaviour and  
392 oxic/suboxic carbon remineralisation processes is usual in marine sediments (Burdige, 2006; Gao et al.,  
393 2009; Teal et al., 2009; 2013). Increasing DGT-iron fluxes near the sediment surface occurred at all

394 stations and there was continued supply to the resin gel at increasing depths. The rate of increase of iron  
395 supply with depth at the disposal stations was greater than at the reference station and is likely to be  
396 driven by the more reducing conditions found at these locations. Iron showed continued supply to depth  
397 whilst Mn showed a subsurface peak.



399

400

401

402 Figure 4: Vertical profiles of metal flux to the DGT probes at the three stations (reference, station C  
 403 and station S) - Fe, Mn, Ni, Pb, Cd. Error bars are +/- 1 standard deviation, n=3

404

405 The peak in the Mn concentration in the subsurface layer is often observed in coastal systems (Gao et  
406 al., 2009; Teal et al., 2013), however, the continued supply of iron to the resin gel with increasing depth,  
407 found in this study, is in contrast to others which show an iron peak (Gao et al., 2006; Merritt and  
408 Amirbahman; 2007). This continued supply at depth could be linked to very low sulphide  
409 concentrations which allow reduced iron to be readily available for uptake by the DGT probes. The  
410 supply rates for Fe and Mn to the resin gel from sediments at the disposal stations were higher than at  
411 the reference station. This is consistent with the higher organic matter loads at the disposal sites and  
412 thus the increased reducing conditions found there. This is also corroborated by the SPI images at the  
413 disposal sites, which show more reducing conditions closer to the sediment surface. The Fe fluxes were  
414 one order of magnitude higher than Mn fluxes. The profile shapes indicate a supply of dissolved Mn  
415 across the Sediment – Water Interface (SWI) into the water column, but this was not observed for iron,  
416 which is probably oxidised within the upper cm of the sediment where oxygen is present. The DGT flux  
417 profiles indicate that the resupply to the resin gel is higher at the disposal sites, despite similar bulk Fe  
418 and Mn levels across the sites.

419

420 **Cadmium:** All 3 stations showed a peak of DGT available cadmium at the SWI. Below the SWI, levels  
421 of Cd supply were low at all stations, apart from distinct peaks of higher Cd supply at discrete depths  
422 (0.1 to 0.2 fmol/cm<sup>2</sup>/s). This release of Cd across the SWI and the maximum in the sediment surface  
423 layer can be attributed to the mobilisation of metal from particles having recently been deposited on the  
424 sediment surface, mainly through the rapid degradation of organic matter accumulated on the surface  
425 of the sediment. This process can be related to break-down of deposited phytodetritus (Fones et al.,  
426 2004; Sakellari et al., 2011) and can also be associated with other metals such as Cu and Zn. There was  
427 no trend of Cd release with increasing depth at any of the stations. The low Cd particulate concentrations  
428 and lack of difference in Cd supply between the reference and disposal stations would imply that Souter  
429 Point stations were not a significant source of Cd release into the pore-water associated with dredged  
430 material disposal, but that it is likely that the SWI Cd source was seasonal deposition and burial of  
431 phytodetrital material.

432

433 **Lead:** Lead (Pb) profiles showed increasing flux to the resin gel with depth, with the flux rate increasing  
434 at all stations in the deeper sediment layers. The fluxes at the reference station and at the disposal station  
435 S were similar, whilst disposal station C showed the highest Pb fluxes (Figure 4).

436 The variability (relative SD) in Pb flux with depth was lower at the reference station and highest at the  
437 disposal stations. This variance was similar to other metals, illustrating the heterogeneity in sediment  
438 conditions and hence metal cycling introduced by dredged material disposal operations. The levels of  
439 total Pb were highest at the disposal station C, but not directly proportionate to the much higher supply  
440 rates observed. This discrepancy showed that mechanisms of metal release could be complex and  
441 therefore cannot be determined from total sediment metal content alone. Indeed, studies have shown



442 that Pb could respond much more to concentrations of organic matter and Acid Volatile Sulphide (AVS)  
443 (Duran et al., 2012) rather than other sediment variables. Both disposal stations show a surface peak in  
444 Pb supply to the resin gel close to the SWI which means that these sites could be acting as sources of  
445 pore-water Pb to the water column. This is not the case at the reference station. It is possible that this  
446 release of Pb (a metal with a high partition co-efficient,  $K_d$ ) within the upper layers of the sediment  
447 could be linked to Fe/Mn particulate reduction. In sub-oxic zones within estuarine sediments, Fe and  
448 Mn can act as master variables controlling the distribution and speciation of other trace elements  
449 (Forstner et al., 1986; Butler et al., 2005).

450

451 **Nickel:** All 3 stations showed an increase in nickel (Ni) supply to the DGT device in the upper few cm  
452 of the sediment, with consistent supply rates at depths greater than 5 cm. This increase is likely to be  
453 linked to the reduction of Fe and Mn oxyhydroxides and degradation of organic material as shown by  
454 the Fe/Mn flux and labile carbon (chlorophyll/phaeopigment) profiles. This behaviour has also been  
455 observed in other DGT studies (Tankere-Muller et al., 2007). The overall supply of Ni to the sediment  
456 pore-water throughout the profile at disposal station C was higher than at the other two stations. It is  
457 likely that the presence/absence of other complexing species (not sulphides) must be creating this  
458 between station heterogeneity of supply to the resin gel, given the consistent total Ni particulate pool.

459 Similar to the observed Pb behaviour, the release of Ni near the SWI can be a source of Ni to  
460 the water column. This was observed at both disposal stations, in contrast to the reference station. For  
461 Ni this could be driven by local release to pore-waters in the upper layers of the sediment (0 to 5 cm  
462 depth).

463

464 **Sulphide:** Metal availability and mobility can be closely linked to the amount of free sulphide ions in  
465 sediments, especially at depth (Gao et al., 2009). Deployment of AgI gel probes into the sediments cores  
466 revealed that free sulphide was at or below the limit of detection for the DGT based method evaluated  
467 through colour scanning. The sulphide detection limit for the AgI gels was 0.25  $\mu\text{mol/L}$  for a 24 hour  
468 deployment which equates well to previous studies (Teasdale et al., 1999). This correlated well with  
469 the high concentrations of free Fe and Mn ions observed in the metal profiles, as any free sulphide  
470 would have reacted with the Fe and Mn to form insoluble iron/manganese-sulphide complexes.

471

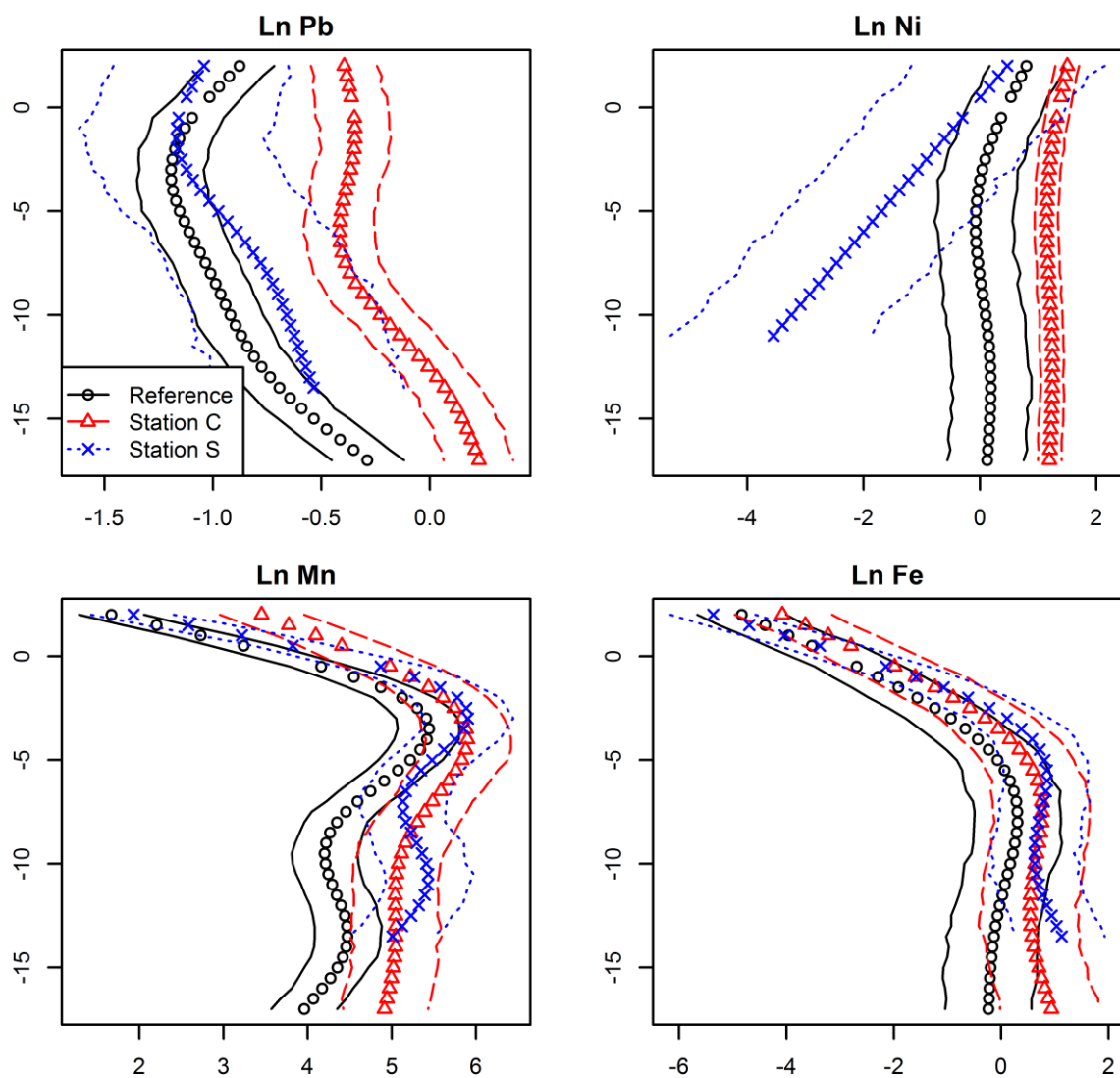
### 472 *3.4 Statistical analysis and comparison of the DGT profiles*

473 Figure A.2 (Appendix 1) shows natural log depth profile plots for all five metals. For Cd, it is difficult  
474 to statistically distinguish the profiles between the stations. For the remaining four metals (Pb, Ni, Mn  
475 and Fe), we used the 95% envelope plots in Figure 5 to further explore differences between the sites.

476 For Mn and Fe we used the 1-lag autocorrelation models (equation (4)) for the residuals to create these  
477 envelopes (see Figure A.3, as an example, to see the autocorrelated residuals for Mn). Note that these

478 models did successfully remove the autocorrelation. For Pb and Ni we used the independence model in  
479 equation (3).

480 For Fe, the envelopes overlap throughout the profile and it is impossible to distinguish the stations from  
481 each other. In contrast, the Ni reference and station C profiles are consistently different, whereas the  
482 station S profile diverges from the other two with increasing depth. Stations S and C (the disposal  
483 stations) have similar profiles for Mn, but the reference station profile separates off slightly from the  
484 other two at depths below about 8cm. The reference and station C profiles are very different for Pb.  
485 However, the large amount of variation for station S makes it difficult to distinguish this station from  
486 the other two statistically.



487  
488 Figure 5: 95% confidence envelopes for the profiles of Ln metal flux to the passive sampler at each  
489 station for Pb, Ni, Mn and Fe

490 In summary, for Mn and Fe the reference station profile is statistically different from the other  
491 two stations, especially at depth, whereas it is difficult to distinguish between the profiles for the other

492 two disposal stations (S and C). For Pb, as previously seen, station C is distinctly different from the  
493 other two stations whereas there is only an obvious difference between profiles for site S and the  
494 reference station at mid depths. For Ni all three stations are different for almost the whole profile with  
495 the reference fluxes lying between lowest fluxes at station S and highest fluxes to the resin gel at site  
496 C. The only exception is near the surface, where station C and the reference station have similar profiles.

497 This analysis is designed to introduce some statistically defensible method to describe and test  
498 differences between DGT profiles in relation to different metals, sites and the impact of an activity such  
499 as dredge material disposal. This can be very useful for regulatory or licensing purposes in comparing  
500 spatial or temporal changes in metal behaviour. The work here illustrates that given the high variability  
501 within some sites it can be difficult to determine statistically the difference between disposal and  
502 reference stations for some metal fluxes. Greater replication (here  $n = 3$  at each station) would improve  
503 the power of such a technique, helping to distinguish reference and impact changes in sediment  
504 conditions for improved disposal site monitoring (over different depth or spatial and temporal  
505 resolutions).

506

### 507 *3.5: Summary of findings and discussion*

508 Dredging and disposal are major activities for sustainable port development and expansion worldwide.  
509 The assessment of the effects of sediment metal contamination, associated with dredging and disposal,  
510 on biological assemblages and function remains a key question in marine management. However, the  
511 appropriate description of bioavailable metal concentrations within pore-waters has rarely been  
512 reported, as routinely only total metal concentrations are monitored. In the majority of targeted  
513 monitoring programmes, where cost-effectiveness and increasing complexity of regulatory questions is  
514 an ever increasing demand, there is an opportunity to incorporate novel approaches which can improve  
515 the information and understanding provided. For example, changing regulatory demands from  
516 understanding metal contamination levels towards biological effects/toxicity and impact assessment  
517 and human activity management. In this work we have attempted to test the use of DGT passive sampler  
518 as means of generating cost-effective (compared to conventional porewater sampling, total metal  
519 analysis at an equivalent resolution or specific bioavailability studies), targeted and novel information  
520 on metal release (sources and sinks) and behaviour within marine sediments.

521 Traditional monitoring of disposal sites within the UK provides the quantitative analysis of total  
522 metal within bulk sediments with limited depth resolution (see Appendix 1 Figure A.1). This is used to  
523 undertake assessments of metal risk posed from a total pool. Many papers have illustrated the lack of  
524 agreement between total metal concentrations and metal availability in the pore-waters and hence  
525 bioavailability and ecotoxicological risk (Di Toro 1992; Lee and Lee, 2005; U.S. EPA, 2005; Roullier  
526 et al., 2008). In comparison, the DGT technique applied in this study has provided higher resolution  
527 depth information on comparative fluxes of metals to the pore-water (primarily via dissolution and/or  
528 desorption of weakly bound metals from the solid phase), and hence potential bioavailability (via

529 various solute pathways). This type of information can describe areas of metal loss/remobilisation with  
 530 depth, contrast the release/resupply of metals between sites and can also illustrate the presence,  
 531 magnitude and direction of metal fluxes across the sediment-water interface. Table 2 summarises each  
 532 of these information types supplied by the DGT (namely, metal behaviours observed at the three sites  
 533 with respect to DGT, Sediment-Water Interface fluxes, and additional information supplied by DGT)  
 534 in comparison to the total metal enrichment information. The implications of these findings are  
 535 discussed further in subsequent sections.

536

537 Table 2. Summary metal behaviour at the 3 disposal site stations as derived by DGT profiles and  
 538 comparison to total bulk metal reservoir (SWI = sediment-water interface)  
 539

<b>Metal</b>	<b>Enriched in disposal sediments</b>	<b>Depth profile shape and flux to DGT</b>	<b>Flux across SWI</b>	<b>Insight given by DGT profiles</b>
<b>Ni</b>	No	Shallow sub-surface peak of Ni release at disposal sites only. Supply to resin gel consistent with depth across all sites. Flux to resin gel higher at station C.	Flux to water column at disposal sites, associated with a shallow sub-surface peak.	Supply of Ni to water column at disposal sites. Pore-water chemistry controls supply to resin gel at station C.
<b>Cd</b>	Yes	Shallow subsurface peak (<1cm) at all sites. Distinct peaks of remobilisation and flux to resin gel. Some LOQ issues. Not coupled to total sediment metal (bulk or profile).	Flux to the water column at all stations, associated with shallow sub-surface peak.	Release not linked to disposal source. Likely phytodetritus source but controls related to redox (Fe/Mn).
<b>Pb</b>	Yes	Increased supply to resin gel with depth. Flux to resin gel significantly higher at station C.	Flux to water column at disposal sites, associated with a shallow sub-surface peak (Pb release from Mn/Fe reduction).	Higher disposal total metal only released at station C. Other factors controlling DGT uptake ( $S^{2-}$ , DOC). Link to Mn or Fe particulate reduction ~ high Pd Kd
<b>Fe</b>	No	Increased Fe supply to resin gel below oxic layer (>1cm). Rate of increase and flux greater at disposal sites. Flux is maintained or increases with depth.	None – oxic layer prevents release.	Higher iron release at disposal sites – linked to increased reducing conditions at depth & elevated TOC. No SWI exchange limited by oxic layer
<b>Mn</b>	Yes	Increased resupply as oxygen saturation decreases.	Flux to the water column at all sites	Release governed by increasingly reducing

	Peak resupply in upper 4 cm and then decline to depth. Flux to the resin gel and depth/rate of increase with depth is higher at the disposal sites.	but higher at disposal sites.	conditions at disposal sites (fines and TOC).
--	---	-------------------------------	---

540

541 *Metal behaviour (release, availability, cycling) information provided by DGT:*

542 Firstly, DGT provides high resolution information with depth DGT flux data inferred to be  
543 DGT-labile metal (dissolved metal present in the pore-water as well as “weakly” bound to the solid  
544 phase), its production within the sediment, release and behaviour, and associated site differences. Iron  
545 and manganese display behaviour consistent with increasingly reducing conditions at depth, i.e.  
546 increased release to the pore-water and availability to DGT. Two of the metals (Pb, Ni) illustrate  
547 subsurface DGT-labile ( $C_{DGT}$ ) peaks (close to the SWI ~ <1cm) which can be a result of increased metal  
548 release from degradation of organic material and/or reduction of Fe and Mn oxyhydroxides associated  
549 with elevated TOC loading associated with disposal activity (i.e. only present or elevated at the disposal  
550 sites). Thus, these disposal sediments represent a source of metal to the overlying water column.  
551 Additionally, the overall increase of metal fluxes observed across the whole sediment profile for Ni and  
552 Pb in the disposal sites (especially in site C) could be evidence that the disposed sediment material may  
553 release larger amounts of DGT-labile (and hence bioavailable) metals in the pore water.

554 Although Cd exhibits similar peaks of DGT flux (DGT-labile metal), the magnitude and depth  
555 distributions of the DGT-Cd fluxes are similar across all sites, despite the elevated bulk total Cd levels  
556 reported at the disposal sites. It is therefore likely that this Cd supply to the pore-water is not related to  
557 disposal activities, but decomposition of Cd enriched phytodetritus, either at the surface, as supported  
558 by the SWI associated peaks (<1cm) or regular peaks of DGT-Cd flux with depth across all of the sites  
559 (reference and disposal) and consistent with frequent and regional bloom deposition and burial events.  
560 Metals such as Cu and Zn have also been shown to exhibit this behaviour (Lee and Morel, 1995; Wang  
561 and Dei, 2001).

562

563 *Linking total metal pool (particulate) and pore-water behaviour:*

564 DGT use also illustrates the lack of agreement between total metal pool determined during routine  
565 monitoring of the disposal activity and the metal concentrations/DGT-labile ( $C_{DGT}$ ) found in pore-  
566 waters as highlighted by the DGT flux. There is clear contrast between the total metal particulate  
567 reservoir and the release for certain metals. The differences in both DGT profile shape and release of  
568 metals in relation to total sediment metal can be seen in Appendix 1, Figure A.1. This is observed in  
569 particular for Cd, which is enriched in bulk sediments at the disposal sites but whose source is likely to  
570 be linked to phytodetrital decomposition (Fones et al., 2004; Sakellari et al., 2011). Pb and Mn also  
571 show enrichment in disposed sediments, but elevated release into the pore-waters is only seen for Mn.

572 For other metals, the DGT data illustrates that release to the pore-waters is controlled by a combination  
573 of redox levels (Fe, Mn) and links to Fe/Mn particulate control on partitioning (Pb).

574 Concentrations of metals in the pore-water can also be controlled by other pore-water phases  
575 such as the presence of Dissolved Organic Carbon (DOC) or Acid Volatile Sulphides (AVS) (especially  
576 Pd, but not Ni) (Lee and Lee, 2005; Duran et al., 2012). It is this control of metal release by and from  
577 pore-water particulate compounds (solid phases / colloidal material) and associated within pore-water  
578 chemistry that will ultimately control the availability of metal to the resin gel as supplied from the  
579 particulate sediment pool (Chifroy et al., 2011). At these sites, free sulphide was below detection limits  
580 in the upper parts of the sediment. The controlling behaviour of  $S^{2-}$  species on metal pore-water supply  
581 is complex and could inhibit/restrict metal release fluxes to a DGT sampler depending on solubility and  
582 the prevailing redox or pH conditions (Ankley et al., 1991; Ankley, 1996a; Lee and Lee 2005; Teal et  
583 al., 2009; Duran et al., 2012). This control of pore-water chemistry on DGT-metal flux can be seen in  
584 the increased release of Pb and Ni to the DGT device at Station C despite no clear relation to drivers  
585 such as the total sediment metal pool. This change is also highlighted in the differing behaviour of Ni  
586 across all three stations despite an equivalent Ni total sediment pool at all sites.

587 The metal pore-water flux profiles determined in this study illustrate the comparative  
588 differences and balance between the metal release from the total particulate pool, pore-water metal  
589 chemistry and hence availability to a pore-water sampler such as DGT. The controls on this release are  
590 complex and relate to dynamic equilibrium interactions between the total metal particulate pool, the  
591 impact of reduction chemistry with depth, and the complexation of released metal ions by pore-water  
592 ligands such as sulphur species or organic matter (Chifroy et al., 2011). These chemical interactions  
593 within the pore-water will ultimately control metal availability to the DGT and hence metal release  
594 within or from the sediment. The understanding of these complex processes is still challenging though  
595 the status information provided by the DGT, as a description of labile/bioavailable metal is useful, even  
596 without a full understanding of the mechanistic drivers.

597

598 *DGT, bioavailability, bioaccumulation and ecotoxicology:*

599 DGT has often been described as a tool capable of describing the bioavailable fraction of metals in  
600 comparison to total metals (Simpson et al., 2007; Simpson et al., 2012; Amato et al., 2015; Ren et al.,  
601 2015). This study has illustrated the capacity for DGT to provide vertically resolved metal fluxes to a  
602 passive sampler, which could be used as a proxy for a bioavailable fraction. The potential disconnection  
603 between total metals and DGT-metal flux observed here has been observed in other studies (see Di  
604 Toro 1992; Roulier et al., 2008), although total metals in sediments were the best predictors of  
605 bioaccumulation in other studies (Roulier et al., 2008 and references there-in). Some studies have  
606 started investigating the links between metal phases (particulate totals, acid extractable, dissolved, DGT  
607 fractions) and biological response/load (Simpson et al., 2012). However, further development to  
608 demonstrate dose/response from DGT fractions and benthic organisms / effects and appropriate solid

609 phase – pore-water phase modelling would be beneficial. In particular, the complex controls on metal  
610 bioavailability created by the interactions within the pore-water chemistry inhibit a mechanistic  
611 understanding of the conditions that will promote metal release from a similar total metal pool. The best  
612 descriptors of bioavailable metal are still being discussed and evaluated under controlled experimental  
613 conditions. An enhanced understanding through combined pore-water metal observational and  
614 modelling approaches is needed to enable predictions or risk assessments of metal bioavailability and  
615 toxicity to be undertaken in the marine environment under contaminated conditions, including disposal  
616 sites.

617 The dynamics between metal supply (particles), metal release and complexation (pore-water)  
618 and uptake (bioavailability or bioaccumulation) is a complex one but can be linked to key variables  
619 (Dissolved Organic Carbon - DOC, Acid Volatile Sulphide - AVS) in future to further understand  
620 release mechanisms and controls. DGT defined fractions may have a role to play here in describing the  
621 potential availability and toxicity of a sediment in a similar way to Simultaneously Extractible Metal  
622 (SEM) : AVS information (Di Toro et al., 1990; 1992; US EPA , 2005; Simpson et al., 2007; Knox et  
623 al., 2012; Simpson et al., 2012 ). A rapid, depth and space integrated imaging technique such as SPI,  
624 which describes iron reduction or sulphide precipitation depths, further aids understanding.

625 The knowledge of the metal release dynamics provided by DGT enhances our ability to describe  
626 and explain different biological uptake or impacts observed in sediments of similar total metal  
627 concentrations and improves the understanding of the links between total metal, pore-water and  
628 biological effects. This description of metal concentration beyond a traditional total measurement is  
629 largely missing in local regulatory or regional scale impact or status assessments within the UK or  
630 Europe such as OSPAR Quality Status Reports (OSPAR QSR 2010) or ICES reports (ICES WGMS).  
631 And yet, improved understanding of the link between hazardous substances and biological responses in  
632 sediments is also required as management regulations increasingly require an ecosystem approach. For  
633 example, the European Union Marine Strategy Framework Directive (2008/58/EC) includes Descriptor  
634 8, which considers the management of sediment contaminant concentrations “*at levels not giving rise*  
635 *to pollution effects*” and requires appropriate linkages of benthic system parameters and anthropogenic  
636 pressures to invoke a management response (Van Hoey et al., 2010; Borja et al., 2013).

637

#### 638 *Considerations for monitoring applications*

639 A main driver of this study has been to assess the utility of a passive sampler such as DGT to provide  
640 better assessment of the risk posed of metal remobilisation from sediments and therefore to aid future  
641 sediment activity management. The case study has demonstrated the feasibility by which such relatively  
642 cost-effective, easy to use techniques can be built into a monitoring programme alongside the other  
643 measures already being sampled. Such a technique can be focused towards site specific contaminant or  
644 management (e.g. capping strategies) issues whilst more rapid techniques such as SPI can provide wider  
645 spatial context (Germano et al., 2011; Birchenough et al., 2013).

646 In combination with monitoring of total sediment metal, DGT is capable of illustrating areas of metal  
647 release, fluxes across the interface and the potential disconnection between total particulate metal pool  
648 and pore-water metal. This is especially useful in describing and quantifying a potential pressure or risk  
649 associated with metal contamination.

650         Critical within a regulatory framework are also methods to demonstrate and track changes  
651 related to an activity, in space/time. This is particularly important for disposal site licensing and  
652 monitoring. It is essential to be able to describe changes in metal levels or behaviour in an auditable  
653 and defensible way. The comparison of metal profiles between sites has usually occurred by visual  
654 comparisons and descriptions, and sometimes regression analysis with depth (Fones et al., 2004).  
655 However, this is not statistically robust or makes site comparison difficult, and with higher variances  
656 induced by natural sediment heterogeneity or disturbance it is essential to have a method that can detect  
657 metal differences within and between sites or changes over time. The statistical modelling of the DGT  
658 metal profiles in this study has demonstrated a methodology that allows statistical analysis and  
659 investigation of high resolution metal profiles. This approach can provide increased confidence in an  
660 assessment of the differences between sites, the site status or processes driving changes in metal levels  
661 and distributions and how disposal is affecting them. Despite the high variance, it provides increased  
662 ability to determine status/metal flux levels statistically and detect changes over depth, time or space.  
663 This is particularly important for detecting changes as a result of a management action or tracking  
664 changes after a management action has been implemented. The power of the technique could be  
665 improved with increased replication and further investigation of variability with space and time.

666         These insights into metal release (by coupling the DGT measurements and statistical  
667 investigation of the profiles) can provide supporting, targeted and complimentary evidence to risk  
668 assessments of metal impact at particular locations or for specific questions. The coupling technique is  
669 compatible with existing monitoring programmes as documented here. It could be directed towards a  
670 specific condition or question highlighted by routine monitoring or total metal assessments. It could  
671 also be used to refine total metal trigger levels through improved understanding of the relationship  
672 between total metal and pore-water concentrations and resupply (flux). The depth information can also  
673 be used to make assessments of metal release risk to the water column under physical disturbances  
674 (storms, trawling). Further work would be needed though to give a greater overview of spatial and  
675 temporal variability in metal behaviour in relation to total sediment metal levels related to disposal  
676 activities and other controlling factors within the sediment matrix, which will dictate metal availability  
677 within the pore-water. Combined with rapid spatial techniques such as SPI it might be possible to  
678 investigate the disposal site signature and associated changes in metal availability and risk of release  
679 under contrasting environmental conditions.

680

681



682 **4.0 Conclusions**

683 The application of high resolution DGT passive samplers to the three sites in this study has improved  
684 our understanding of specific metal remobilisation behaviour, contrasting release features between  
685 metals, sites and with depth. It has also demonstrated that total particulate metal and DGT-metal flux  
686 are not always in agreement, indeed, elevated total particulate metal concentrations do not necessarily  
687 lead to high metal release into the sediment pore-waters. This initial application of DGT passive sampler  
688 technology, alongside sediment bulk metal analysis, to evaluate metal behaviour at the Souter Point  
689 disposal site has highlighted the complex relationship between contaminant disposal load from  
690 particulates and metal availability to the pore-water. Furthermore, it has underlined the metal  
691 heterogeneity found in the sediments at this disposal site, both between stations and with depth.

692 While bulk sediment analysis for metals gives important information about the quantity of  
693 metals present, i.e. the size of the benthic reservoir, and is indicative of the potential hazard, it does not  
694 give information about the availability of these metals to the various components of the ecosystem and  
695 thus the actual risk posed – either to the benthic community or by flux into the overlying water column  
696 and so into the pelagic system. This is where complementary methodology such as DGT enables  
697 additional insights. The clear differences in metal flux profiles recorded at different stations, which do  
698 not strictly correlate with total metal concentrations in the corresponding slices, illustrate that  
699 environmental parameters are influential in regulating fluxes and, by implication, availability of metals.  
700 Statistical modelling approaches, as documented here, could be developed in future to describe and  
701 track changes in metal behaviour and release across areas and also mechanistically with other metal  
702 (metal:metal couples) or environmental controls.

703 In summary, the use of depth resolving passive samples such as DGT is compatible with routine  
704 monitoring of disposal sites and can provide valuable additional information. Further work to improve  
705 understanding of the controlling factors of metal release to pore-waters, and the likely exposure routes  
706 of biota (linked to faunal traits such as feeding modes or sediment location) within the receiving  
707 ecosystem as well as corresponding ecotoxicological implications would be beneficial to inform  
708 management decisions. Such an increased understanding would not only enable more robust  
709 assessments of risks posed by disposal of sediments with high contaminant loads, but could also be used  
710 when assessing likely impacts arising from natural events, such as storms, and human activities, such  
711 as fishing and changes in controlling parameters under predicted future climate scenarios.

712

713 **Acknowledgements:**

714 This work was supported by Defra and MMO (contract E5403). The views expressed are those of the  
715 authors and do not reflect the policies of the funding departments. We gratefully acknowledge the  
716 valuable contributions made by the scientific staff and crew of the RV Cefas Endeavour. We also thank

717 Robin Law and three anonymous reviewers for comments to really improve the manuscript and insights  
718 our data provided.

719

720 **References:**

721

722 Amato, E.D., Simpson, S.L., Jarolimek, C.V., Jolley, D.F. Diffusive Gradients in Thin Films Technique  
723 Provide Robust Prediction of Metal Bioavailability and Toxicity in Estuarine Sediments. *Environ. Sci.*  
724 *Technol.*, 2014; 48 (24), 4485–4494.

725

726 Amato, E.D., Simpson, S.L., Belzunce-Segarra, M.J., Jarolimek, C.V., Jolley, D.F. Metal Fluxes from  
727 Porewaters and Labile Sediment Phases for Predicting Metal Exposure and Bioaccumulation in Benthic  
728 Invertebrates. *Environ. Sci. Technol.*, 2015; 49, 14204–14212.

729

730 Ankley, G.T., Phipps, G.L., Leonard, E.N., Kosian, P.A., Cotter, A.M., Dierkes, J.R. Acid-volatile  
731 sulfide as a factor mediating cadmium and nickel bioavailability in contaminated sediments. *Environ*  
732 *Toxicol Chem* 1991; 10:1299– 307.

733

734 Ankley, G.T. Evaluation of metal/acid-volatile sulfide relationship in the prediction of metal  
735 bioaccumulation by benthic macroinvertebrates. *Environ Toxicol Chem* 1996a; 15:2138– 46.

736

737 Ankley, G.T., Di Toro, D.M., Hansen, D.J., Berry, W.J. Technical basis and proposal for deriving  
738 sediment quality criteria for metals. *Environ Toxicol Chem* 1996b; 15:2056– 66.

739

740 Birchenough, A., Bolam, S.G., Bowles, G.M., Hawkins, B. Whomersley, P., Weiss, L. Monitoring of  
741 dredged material disposal sites at sea and how it links to licensing decisions. *Proceedings from PIANC*  
742 *MMX*, Liverpool, May 2010.

743

744 Birchenough, S.N.R., Boyd, S.E., Coggan, R.A., Limpenny, D.S., Meadows, W.J., Rees, H.L. Lights,  
745 camera and acoustics: Assessing macrobenthic communities at a dredged material disposal site off the  
746 North East coast of the UK. *Journal of Marine Systems* 2006; 62 (3): 204-216.

747

748 Birchenough, S.N.R., Blake, S.J., Rees, J., Murray, L.A., Mason, C.E., Rees, H.L., Vivian, C.,  
749 Limpenny, D.S. Contaminated dredged material: monitoring results from the first capping trial in the  
750 U.K. In: 4th International Conference: Proceedings of the Port Development and Coastal Environment.  
751 25–28 September 2007, Varna Bulgaria.

752

753 Birchenough, S.N.R., Bolam, S.G., Parker, E.R. SPI-ing on the seafloor: characterising benthic systems  
754 with traditional and in situ observations. *Biogeochemistry* 2013; 113 (1-3): 105-11  
755

756 Bolam, S.G., Rees, H.L., Somerfield, P., Smith, R., Clarke, K.R., Warwick, R.M., Atkins, M.,  
757 Garnacho, E. Ecological consequences of dredged material disposal in the marine environment: a  
758 holistic assessment of activities around the England and Wales coastline. *Marine Pollution Bulletin*  
759 2010a; 52: 415-426.  
760

761 Bolam, S.G., Mason, C., Bolam, T., Whomersley, P., Birchenough, S.N.R, Curtis, M., Birchenough,  
762 A., Rumney, H., Barber, J., Rance, J., McIlwaine, P., Law, R.J., Dredged material disposal site  
763 monitoring around the coast of England: results of sampling. SLAB5 Project Report, Cefas, UK. 2010b.  
764

765 Borja, A., Elliott, M., Marine monitoring during an economic crisis: the cure is worse than the disease.  
766 *Mar. Pollut. Bull.* 2013; 68: 1–3.  
767

768 Bufflap, S. E., Allen, H. E. Sediment pore water collection methods for trace metal analysis: A review.  
769 *Wat. Res.* 1995; 1: 165-177  
770

771 Bull, D.C., Williamson, R.B. Prediction of principal metal-binding solid phases in estuarine sediments  
772 from colour image analysis. *Environ. Sci.Technol.* 2001; 35:1658-1662.  
773

774 Burdige, D.J. *Geochemistry of marine sediments.* Princeton University Press. 2006.  
775

776 Butler, E., Leeming, R., Watson, R., Armand, S., Green, M., Final Report on Sediment Resuspension  
777 Experiment for Derwent CCI Project. CSIRO Marine Research, Hobart, Tasmania, Australia.  
778 <http://www.derwentestuary.org.au/file>. 2005.  
779

780 Calmano, W., Hong, J., Forstner, U. Binding and mobilisation of heavy metals in contaminated  
781 sediments affected by pH and redox potential. *Water Sci Technol* 1993; 28: 223–35.  
782

783 Chapman, P.M., Wang, F., Janssen, C., Persoone, G., Allen, H.E. Ecotoxicology of metals in aquatic  
784 sediments: binding and release, bioavailability, risk assessment, and remediation.  
785 *Can J Fish Aquat Sci* 1998; 55: 2221–43.  
786

787 Ciffroy, P., Nia, Y., Garnier, J.M. Probabilistic Multicompartmental Model for Interpreting DGT  
788 Kinetics in Sediments. *Environ Sci Technol* 2011; 45: 9558–9565.  
789

790 Dahlqvist, R., Zhang, H., Ingri, J. and Davison, W. Performance of the diffusive gradients in thin films  
791 technique for measuring Ca and Mg in freshwater. *Anal Chim Acta* 2002; 460(2): 247-256.  
792

793 Davison, W., Zhang, H. In situ speciation measurements of trace components in natural waters using  
794 thin-film gels. *Nature* 1994; 367: 546–8.  
795

796 Davison, W., Fones, G. R. & Grime, G. W. Dissolved metals in surface sediment and a microbial mat  
797 at 100- $\mu$  m resolution. *Nature* 1997; 387, 885-888.  
798

799 Davison, W., Zhang, H. Progress in understanding the use of diffusive gradients in thin films (DGT) –  
800 back to basics. *Environ. Chem.* 2012; 9: 1–13.  
801

802 Davison, W., Fones, G.R., Harper, M., Teasdale, P., Zhang, H. Dialysis, DET and DGT: in situ  
803 diffusional techniques for studying water, sediments and soils. In: Buffle, J., Horvai, G. (Eds.), *In-Situ*  
804 *Monitoring of Aquatic Systems: Chemical Analysis and Speciation*. IUPAC. Wiley, New York, 2000;  
805 495–569.  
806

807 Davison, W., Zhang, H., Warnken, K.W. Theory and applications of DGT measurements in soils and  
808 sediments. In: Greenwood, R., Mills, G., Vrana, B. (Eds.), *Comprehensive Analytical Chemistry*.  
809 *Passive Sampling Techniques in Environmental Monitoring*, Elsevier, 2007; 48: 353–378.  
810

811 Di Toro, D.M., Mahony, J.D., Hansen, D.J., Scott, K.J., Hicks, M.B., Mayer, S.M., Redmond, M.S.  
812 Toxicity of cadmium in sediments: the role of acid volatile sulfide. *Environ Toxicol Chem* 1990;  
813 9:1489– 504.  
814

815 Di Toro, D.M., Mahony, J.D., Hansen, D.J., Scott, K.J., Carlson, A.R., Ankley, G.T. Acid volatile  
816 sulfide predicts the acute toxicity of cadmium and nickel in sediments. *Environ. Sci. Technol.* 1992; 26:  
817 96–101.  
818

819 Duran, I., Sanchez-Marin, P., Beiras, R. Dependence of Cu, Pb and Zn remobilization on  
820 physicochemical properties of marine sediments. *Mar Environ Res* 2012; 77: 43-49.  
821

822 Directive 2008/56/EC of the European Parliament and of the Council of 17 June 2008 establishing a  
823 framework for community action in the field of marine environmental policy (Marine Strategy  
824 Framework Directive).  
825

826 Eggleton, J., Thomas, K.V. A review of factors affecting the release and bioavailability of contaminants  
827 during sediment disturbance events. *Environ Int* 2004; 30: 973–980.  
828

829 Folk, R.L., 1954. The distinction between grain size and mineral composition in sedimentary rock  
830 nomenclature. *Journal of Geology* 62 (4), 344-359  
831

832 Fones, G.R., Davison, W., Holby, O., Jorgensen, B.B. and Thamdrup, B. High-resolution metal  
833 gradients measured by in situ DGT/DET deployment in Black Sea sediments using an autonomous  
834 benthic lander. *Limnol Oceanogr* 2001; 46(4): 982-988.  
835

836 Fones, G.R, Davison W., Hamilton-Taylor, J. The fine-scale remobilization of metals in the surface  
837 sediment of the North-East Atlantic. *Cont Shelf Res* 2004; 24: 1485–1504  
838

839 Forstner, U., Wittman, G.T.W. Metal pollution in the aquatic environment. Berlin:  
840 Springer-Verlag; 1981.  
841

842 Forstner, U., Ahlf, W., Calmano, W., Kersten, M., Salomons, W. Mobility of heavy metals in dredged  
843 harbour sediments. In: Sly PG, editor. *Sediments and Water Interactions*.  
844 New York: Springer-Verlag. 1986; 371–80.  
845

846 Gao, Y., Leermakers, M., Gabelle, C., Divis, P., Billon, G., Ouddane, B., High resolution profiles of  
847 trace metals in the pore waters of riverine sediment assessed by DET and DGT. *Sci Total Environ* 2006;  
848 362: 266-277.  
849

850 Gao, Y., Lesven, L., Gillan, D., Sabbe, K., Billon, G., De Galan, S., Elskens, M., Baeyens, W.,  
851 Leermakers, M. Geochemical behaviour of trace elements in sub-tidal marine sediments of the Belgian  
852 coast. *Mar Chem* 2009; 117: 88-96.  
853

854 Germano JD, Rhoads DC, Valente RM, Carey DA, Solan M. The use of sediment profile imaging (SPI)  
855 for environmental impact assessment and monitoring studies: lessons learned from the past four  
856 decades. *Oceanogr Mar Biol* 2011; 49:235–298  
857

858 Harper, M.P., Davison, W., Zhang, H. and Tych, W. Kinetics of metal exchange between solids and  
859 solutions in sediments and soils interpreted from DGT measured fluxes. *Geochim Cosmochim Ac* 1998;  
860 62(16): 2757-2770.  
861

862 Harper, M.P., Davison, W. and Tych, W. Estimation of pore water concentrations from DGT profiles:  
863 A modelling approach. *Aquat Geochem* 1999; 5(4): 337-355.  
864

865 ICES Reports from WGMS, accessed on 22<sup>nd</sup> April 2016, URL:  
866 <http://www.ices.dk/community/groups/Pages/WGMS.aspx>  
867

868 Knox, A., Paller, M., Roberts, J. Active Capping Technology—New Approaches for *In Situ*  
869 Remediation of Contaminated Sediments. *Remediation* 2012; DOI: 10.1002/rem.21313.  
870

871 Knox, A. S., Paller, M. H., Milliken, C. E., Redder, T. M., Woolfe, J. R., Seaman, J. Environmental  
872 impact of ongoing sources of metal contamination on remediated sediments. *Sci Total Environ* 2016;  
873 563-564: 108-117.  
874

875 Lee, J., Morel, F.M. Replacement of zinc by cadmium in marine phytoplankton. *Mar Ecol Prog Ser*  
876 1995; 127: 305-309.  
877

878 Lee, J.-S., Lee, J.-H. Influence of acid volatile sulfides and simultaneously extracted metals on the  
879 bioavailability and toxicity of a mixture of sediment-associated Cd, Ni, and Zn to polychaetes *Neanthes*  
880 *arenaceodentata*. *Sci Total Environ* 2005; 338: 229– 241  
881

882 Lyle, M. The brown-green colour transition in marine sediments: A marker of the Fe(III)–Fe(II) redox  
883 boundary, *Limnol. Oceanogr* 1983; 28, 1026–1033.  
884

885 Manly, F. J. Randomization, Bootstrap and Monte Carlo Methods in Biology: 2<sup>nd</sup> edition. Chapman and  
886 Hall, London. 2008  
887

888 Mason, C. NMBAQC's Best Practice Guidance. Particle Size Analysis (PSA) for Supporting Biological  
889 Analysis. National Marine Biological AQC Coordinating Committee, 72pp, Dec. 2011.  
890

891 Merritt, K.A., Amirbahman, A. Mercury dynamics in sulfide-rich sediments: Geochemical influence on  
892 contaminant mobilization within the Penobscot River estuary, Maine, USA *Geochim Cosmochim Acta*.  
893 2007; 71: 929–941.  
894

895 MEMG Group Co-ordinating Sea Disposal Monitoring. Final Report of the Dredging and Dredged  
896 Material Disposal Monitoring Task Team. Science Series Aquatic Environmental Monitoring Reports,  
897 CEFAS, Lowestoft, (55): 52pp. 2003  
898

899 Oporto, C., Smolders, E., Degryse, F., Verheyen, L. and Vandecasteele, C. DGT-measured fluxes  
900 explain the chloride-enhanced cadmium uptake by plants at low but not at high Cd supply. *Plant Soil*  
901 2009; 318(1-2): 127-135.

902

903 OSPAR. Quality Status Report (QSR) 2010. OSPAR Commission, London, 2010: 176 pp.

904

905 Panther, J.G., Bennett, W.W., Welsh, D.T. and Teasdale, P.R. Simultaneous Measurement of Trace  
906 Metal and Oxyanion Concentrations in Water using Diffusive Gradients in Thin Films with a Chelex-  
907 Metsorb Mixed Binding Layer. *Anal Chem* 2014; 86(1): 427-434.

908

909 Peijnenburg, W. J. G. M., Teasdale, P. R., Reible, D., Mondon, J., Bennett, W. W., Campbell, P. G. C.  
910 Passive sampling methods for contaminated sediments: State of the science for metals. *Integrated*  
911 *Environmental Assessment and Management*. 2014; 10(2): 179–196.

912

913 R Development Core Team. R: a language and environment for statistical computing. R Foundation  
914 for Statistical Computing, Vienna, Austria. ISBN 3-900051-07-0, <http://www.R-project.org>. 2010

915

916 Rabouille, C., Denis, L., Dedieu, K., Stora, G., Lansard, B., Grenz, C. Oxygen demand in coastal marine  
917 sediments: comparing in situ microelectrodes and laboratory core incubations *J Exper Mar Biol Ecol*  
918 2001; 285/286: 49–69.

919

920 Rees, H.L., Pendle, M.A., Limpenny, D.S., Mason, C.E., Boyd, S.E., Birchenough, S., Vivian,  
921 C.M.G. Benthic responses to sewage-sludge disposal and climate events in the Western North Sea. *J.*  
922 *Mar. Biol. Assoc. UK*. 2006; 86: 1–18.

923

924 Ren, J., Williams, P.N., Luo, J., Ma, H., Wang, X. Sediment metal bioavailability in Lake Taihu, China:  
925 evaluation of sequential extraction, DGT, and PBET techniques. *Environmental Science and Pollution*  
926 *Research*. 2015; 22 (17), 12919-12928.

927

928 Rhoads, D.C., Germano, J.D. Characterization of organism-sediment relations using sediment profile  
929 imaging: an efficient method of remote ecological monitoring of the seafloor. *Mar Ecol Prog Ser* 1982;  
930 8:115-128

931

932 Roulier, J.L., Tusseau-Vuillemin, M.H., Coquery, M., Geffard, O., Garric, J. Measurement of dynamic  
933 mobilization of trace metals in sediments using DGT and comparison with bioaccumulation in  
934 *Chironomus riparius*: First results of an experimental study. *Chemosphere* 2008; 70: 925–932.

935

936 Rowlatt, S.M., Rees, H.L., Limpenny, D.S. & Allen, J. Sediment quality of the north-east coast of  
937 England. International Council for the Exploration of the Sea (CM Papers and  
938 Reports) 1989; CM1989/E:16, 21pp.  
939

940 Rowlatt, S.M., Ridgeway, I.M. Final reports of the metals task team and the organics task team. Science  
941 Series, Aquatic Environment Monitoring Report, Cefas, Lowestoft, 1997; No. 49,  
942 51 pp.  
943

944 Sakellari, A., Plavsi, M., Karavoltzos, S., Dassenakis, M., Scoullou, M. Assessment of copper,  
945 cadmium and zinc remobilization in Mediterranean marine coastal sediments. *Estuar Coast Shelf Sci*  
946 2011; 91: 1-12.  
947

948 Sapp, M., Parker, E.R., Teal, L.R., Schratzberger, M. Advancing the understanding of biogeography-  
949 diversity relationships of benthic microorganisms in the North Sea. *FEMS Microbiol Ecol* 2010; 74:  
950 410-429.  
951

952 Scally, S., Davison, W., Zhang, H. Diffusion coefficients of metals and metal complexes in hydrogels  
953 used in diffusive gradients in thin films, *Anal. Chim. Acta* 2006; 558: 222-229.  
954

955 Schintu, M., Marras, B., Durante, L., Meloni, P. and Contu, A. Macroalgae and DGT as indicators of  
956 available trace metals in marine coastal waters near a lead-zinc smelter. *Environ Monit Assess* 2010;  
957 167(1-4): 653-661.  
958

959 Shiva, A.H., Teasdale, P.R., Bennett, W.W. and Welsh, D.T. A systematic determination of diffusion  
960 coefficients of trace elements in open and restricted diffusive layers used by the diffusive gradients in  
961 a thin film technique. *Anal Chim Acta* 2015; 888: 146-154.  
962

963 Shiva, A.H., Bennett, W.W., Welsh, D.T. and Teasdale, P.R., 2016. In situ evaluation of DGT  
964 techniques for measurement of trace metals in estuarine waters: a comparison of four binding layers  
965 with open and restricted diffusive layers. *Environ Sci Proc Imp* 2016; 18(1): 51-63.  
966

967 Simpson, S. L., Batley, G. E. Predicting metal toxicity in sediments: A critique of current approaches.  
968 *Integr. Environ. Assess. Manage.* 2007; 3, 18–31.  
969

970 Simpson, S. L., Yverneau, H., Cremazy, A., Jarolimek, C. V., Price, H., Jolley, D. F. DGT-induced  
971 copper flux predicts bioaccumulation and toxicity to bivalves in sediments with varying properties.  
972 *Environm Sci Technol* 2012; 46 (16): 9038-9046.



973 Stockdale, A., Davison, W., Hao, Z. Micro-scale biogeochemical heterogeneity in sediments: A review  
974 of available technology and observed evidence. *Earth-Sci Rev* 2009; 92: 81-97.  
975

976 Tankere-Muller, S., Zhang, H. Fine scale remobilisation of Fe, Mn, Co, Ni, Cu and Cd in contaminated  
977 marine sediment. *Mar Chem* 2007; 106 (1-2): 192-207.  
978

979 Teal, L. R., Parker, R., Fones, G., Solan, S. Simultaneous determination of in situ vertical transitions of  
980 color, pore-water metals, and visualisation of infaunal activity in marine sediments. *Limnol Oceanol*  
981 2009; 54 (5): 1801-1810.

982 Teal, L.R., Parker, E.R., Solan, M. Sediment mixed layer as a proxy for benthic ecosystem process and  
983 function *Mar. Ecol. Prog. Ser* 2010; 298: 79–94.  
984

985 Teal, L.R., Parker, E.R.; Solan, M. Coupling bioturbation activity to metal (Fe and Mn) profiles in situ.  
986 *Biogeosciences* 2013; 10: 2365 – 2378.  
987

988 Teasdale, P.R., Hayward, S., Davison, W. In situ, high-resolution measurement of dissolved sulfide  
989 using diffusive gradients in thin films with computer-imaging densitometry. *Anal Chem* 1999; 71:  
990 2186–2191.  
991

992 Turner, G. S. C., Mills, G. A., Teasdale, P. R., Burnett, J. L., Amos, S. & Fones, G. R. Evaluation of  
993 DGT techniques for measuring inorganic uranium species in natural waters: Interferences, deployment  
994 time and speciation. *Anal Chim Acta* 2012; 739: 37-46.  
995

996 Turner, G. S. C., Mills, G. A., Bowes, M. J., Burnett, J. L., Amos, S. & Fones, G. R. Evaluation of DGT  
997 as a long-term water quality monitoring tool in natural waters; uranium as a case study. *Environ Sci*  
998 *Proc Imp* 2014; 16(3): 393-403.  
999

1000 U.S. EPA. Procedures for the Derivation of Equilibrium Partitioning Sediment Benchmarks  
1001 (ESBs) for the Protection of Benthic Organisms: Metal Mixtures (Cadmium, Copper, Lead,  
1002 Nickel, Silver and Zinc). EPA-600-R-02-011. Office of Research and Development. Washington,  
1003 DC 20460 2005.  
1004

1005 Van Hoey, G., Borja, A., Birchenough, S., Buhl-Mortensen, L., Degraer, S., Fleischer, D., Kerckhof,  
1006 F., Magni, P., Muxika, I., Reiss, H., Schroder, A. & Zettler, M. L. The use of benthic indicators in  
1007 Europe: From the Water Framework Directive to the Marine Strategy Framework Directive. *Mar Poll*  
1008 *Bull* 2010; 60, 2187-2196.

1009 Verardo, D.J., Froelich, P.N., McIntyre, A. Determination of organic carbon and nitrogen in marine  
1010 sediments using the Carlo Erba NA-1500 analyzer. *Deep-Sea Res* 1990; 37: 157–165.  
1011

1012 Wang, W.-X., Dei, R.C. Metal uptake in a coastal diatom influenced by major nutrients (N, P and Si)  
1013 *Wat Res* 2001; 35 (1): 315-321.  
1014

1015 Wood, S.N. *Generalized Additive Models: An Introduction with R*. Chapman and Hall/CRC, London.  
1016 2006.  
1017

1018 Zhang, H., Davison, W., Miller, S. and Tych, W. In-situ high-resolution measurements of fluxes of Ni,  
1019 Cu, Fe, and Mn and concentrations of Zn and Cd in porewaters by DGT. *Geochim Cosmochim Ac*  
1020 1995; 59(20): 4181-4192.  
1021

1022 Zhang, H. and Davison, W. Diffusional characteristics of hydrogels used in DGT and DET techniques.  
1023 *Anal Chim Ac* 1999; 398(2-3): 329-340.  
1024

1025 Zhang, H. and Davison, W. Direct in situ measurements of labile inorganic and organically bound metal  
1026 species in synthetic solutions and natural waters using diffusive gradients in thin films. *Anal Chem*  
1027 2000; 72(18): 4447-4457.  
1028  
1029